Supplemental Data

Mesothelial cells promote early ovarian cancer metastasis through fibronectin secretion

Hilary A. Kenny[1], Chun-Yi Chiang[1], Erin A. White[1], Elizabeth M. Schryver[1], Mohammed Habis[1], Iris L. Romero[1], Andras Ladanyi[1], Carla V. Penicka[1], Joshy George[2], Karl Matlin[3], Anthony Montag[4], Kristen Wroblewski[5], S. Diane Yamada[1], Andrew P. Mazar[6], David Bowtell[2], and Ernst Lengyel[1]

[1]Department of Obstetrics and Gynecology/Section of Gynecologic Oncology, [3]Department of Surgery and [4]Department of Pathology, [5]Department of Health Studies, University of Chicago, Chicago, Illinois, USA
[2]Peter MacCallum Cancer Centre, East Melbourne and Departments of Pathology and Biochemistry and Molecular Biology, University of Melbourne, Melbourne, Australia
[6]Chemistry of Life Processes Institute Northwestern University, Evanston, Illinois, USA

Supplemental Methods

Reagents. Fibronectin was purchased from BD Biosciences. The human ovarian cancer (OvCa) cell lines, SKOV3ip1 and HeyA8, were provided by Dr. Gordon B. Mills (M.D. Anderson Cancer Center). RKO, a human colon carcinoma cell line, was purchased from ATCC (1). The Kuramochi, Tyk-nu and Tyk-nu CP-r cells were purchased from the Japanese Collection of Research Bioresources. The cell lines were validated by short tandem repeat DNA fingerprinting using the AmpFℓSTR Identifier kit (Applied Biosystems) and compared with known American Type Culture Collection fingerprints, the Cell Line Integrated Molecular Authentication database (CLIMA), and the University of Texas MD Anderson Cancer Center fingerprint database. Negative control and fibronectin siRNA were purchased from Ambion Inc., while Smad3 and TGF-β1 siGENOME siRNA were purchased from Darmacon. TGF-β1 was from Gibco. The TGF-βRI kinase inhibitor I (TGF-βRI inhibitor, catalog number 616451) (2), TGF-βRI kinase inhibitor II [TGF-βRI(II) inhibitor, catalog number 616452] (3) and the Rho kinase inhibitor (Rho inh, catalog number 555552) (4) were from Calbiochem. The Ras signaling activity inhibitor (Ras inhibitor, catalog number 10010501) (5) was purchased from Cayman Chemical. The Rac-GEF interaction inhibitor (Rac inhibitor, catalog number 2161) was from Tocris Bioscience (6). The fibronectin antibody (clone 568) was purchased from Millipore. The TGF-βRII antibody (catalog number AF-241-NA) was from R&D Systems. The β_1-integrin (clone P5D2) antibody was purchased from Santa Cruz. The fibronectin antibody (clone 568), β_4-integrin (clone ASC-3), $\alpha_V\beta_3$-integrin (clone LM609) and α_5-integrin (clone P1D6) antibodies were purchased from Millipore. Anti-Smad2/3 (catalog number 610842) and anti-E-cadherin (catalog number 610181) antibodies were from BD Transduction Laboratories. Anti-vimentin (clone V9) antibody was purchased from Dako Cytomation. Anti-actin, anti-pSmad2/3 (clone D6G10) and anti-GAPDH (clone 14C10) antibodies were from Cell Signaling Technology. Ad5CMVCre-eGFP and Ad5CMV-eGFP were purchased from University of Missouri.

Tissue Microarray and Immunohistochemistry. Tissue microarray cores (n=2) of omental metastases from 108 patients with serous papillary OvCa were collected. The patients had undergone surgery performed by a Gynecologic Oncologist at the University of Chicago, and samples were selected by a Gynecologic Pathologist (A. Montag). Clinical and histopathologic information was collected and updated as previously reported (7).

Tissue microarray slides were deparaffinized and incubated with anti-fibronectin (Sigma-Aldrich) at a 1:400 dilution as previously described (8, 9). The slides were stained using the Envision avidin–biotin-free detection system and counterstained with hematoxylin. Quantification and localization of fibronectin protein expression was performed using Aperio ImageScope and Spectrum software. Tumor and stroma specific classifiers were developed using a Spectrum analysis program with Genie capabilities (Supplemental Figure 7). The intensity of DAB staining was determined in tumor or stroma specific regions of the tumor cores.

Differences between tumor and stroma fibronectin expression were evaluated using a Wilcoxon rank test comparing the two treatments.

Omental samples from FIGO Stage IIIA serous papillary ovarian cancer patients were obtained. The patients had undergone surgery performed by a Gynecologic Oncologist at the University of Chicago, and samples were selected by a Gynecologic Pathologist (A. Montag) after obtaining IRB approval. The omental tissues were paraffin embedded slices collected on glass slides. The tissue slides were deparaffinized and stained with Hematoxylin and Eosin.

ECM Isolation. Specimens of human omentum were obtained from patients undergoing surgery for benign conditions under a protocol approved by the University of Chicago Institutional Review Board (IRB). ECM was isolated from primary human omentum obtained from surgery for benign conditions and omental metastases from OvCa patients as previously described (10). Briefly, fresh tissue was cut (1-2mm in thickness), suspended in dispase solution (100 units/g of tissue) and incubated for 2 hours at 4ºC. The tissue sections were rubbed over a cell sieve, and the remaining matrices were homogenized in high salt buffer (0.05M Tris pH 7.4, 3.4 M NaCl, 4uM N-ethylmaleimide) containing protease inhibitors (0.001mg/ml pepstatin, 0.01 mg/ml aprotonin, 2mM orthovanadate, and 1mM PMSF). The martrices were centrifuged three times at 7000g for 15 minutes, and the supernatant was discarded. The pellet was incubated in 2M urea buffer (0.15M NaCl and 0.05 Tris pH7.4) at 1mL of buffer/g tissue rotating for 48 hours at 4ºC. The solubilized ECMs were centrifuged at 14000g for 20 minutes, and supernatant collected. The concentration and sizes of ECMs isolated were analyzed using BCA protein concentration assay and SDS-PAGE. The protocol was adapted from Abberton KM *et al*. (11).

In addition, the ECM secreted by mesothelial cells was analyzed. Briefly, the cells were washed 3 times with PBS and floated off the plate in 0.2N NH_4OH. The remaining ECMs were washed 3 times with PBS, collected and analyzed using SDS-PAGE. The protocol was adapted from (12).

Quantitative Real-Time Reverse Transcription PCR. After co-culture of GFP-labeled OvCa cells with full human omentum, the 3D omental culture or primary human mesothelial cells, cells were sorted by fluorescently-activated cell sorting (FACS) in PBS (8). This procedure separated labeled OvCa cells from mesothelial cells and/or fibroblasts after their co-culture. Trizol reagent was used to isolate RNA according to manufacturer instructions (Invitrogen). cDNA was synthesized using the Applied Biosystems cDNA archive kit. After reverse transcription, real-time PCR was performed using a Prism7500 TaqMan PCR detector (Applied Biosystems) with pre-designed and validated TaqMan probes for fibronectin and TGFβ-1 in conjunction with GAPDH for normalization (Applied Biosystems) (10). The reactions were run in triplicate. Relative levels of mRNA gene expression were calculated using the $2^{-\Delta\Delta CT}$ method (13). Differences between treatments were evaluated using an unpaired, two-tailed Student's t-test.

Immunoblot Analysis. For analysis of cellular fibronectin, tissue or cells were lysed after FACS sorting, and equal quantities of protein were added to each blot. For analysis of secreted ECM, equal volumes of ECM lysates were added to each blot. For analysis of tumor ECM, equal quantities of protein were added to each blot. For analysis of ascites levels of fibronectin, equal quantities of protein were added to each blot. Proteins were resolved by SDS-PAGE, transferred to nitrocellulose and immunoblot analysis performed (10). The following dilutions of antibodies were applied overnight at 4°C: anti-fibronectin (1:2000), anti-E-cadherin (1:2000), anti-GAPDH (1:2000), and mouse anti-actin (1:50,000). The blots were than incubated with secondary horseradish peroxidase-conjugated IgG and visualized with enhanced chemiluminescence reagents.

Primary Omental Mesothelial Cell Culture and imaging. Specimens of human omentum were obtained from patients undergoing surgery for benign conditions. Primary human mesothelial cells were isolated from the omentum, peritoneal wall (peritoneum) or fallopian tube serosa and purification was verified by vimentin and keratin 8 immunohistochemistry (8, 9). Experiments were performed with primary human mesothelial cells at a density of 20,000 cells in 0.33cm^2. The primary human mesothelial cells were imaged using plastic DIC, a wide-field microscope (20x objective) and a CCD camera.

Proliferation Assay. Fluorescently-labeled OvCa cells ($2x10^4$) were plated in a 96-well dish (14). The cells were treated with mouse IgG, β_1-integrin, α_5-integrin, $\alpha_v\beta_3$-integrin or β_4-integrin antibodies (20µg/ml) 24h post seeding. The number of proliferating OvCa cells was measured using a standard curve and a fluorescent plate reader.

Fibronectin Floxed Mouse Experiments. Mice carrying a 'floxed' fibronectin gene ($FN^{fl/fl}$), which have been previously described, were generated by Dr. Reinhardt Fässler (15, 16) and were received from Dr. Sarah Dallas at the University of Missouri-Kansas City, Missouri. The mice were bred in house and genotyped as described below. Homozygous floxed fibronectin mice have no reported or observed abnormalities. The mice are fertile and have a normal lifespan.

In order to generate mice with tissue-specific deletion of the fibronectin gene, Cre must be expressed in a tissue-specific and/or inducible manner (15). Therefore, peritoneal surface cells were isolated and cultured from the $FN^{fl/fl}$ mice. The peritoneal surface cells received adenovirus encoding Cre recombinase (Ad5CMVCre; adeno-Cre) to delete fibronectin or empty control adenovirus (Ad5CMV; adeno-Cont) treatment for 72 h prior to fibronectin production stimulation with TGF-β1 (2μg/ml) for 48 h. The adenovirus infection was efficient (>92%, infection at a MOI of 50) as observed with eGFP expression and did not reduce viability (at MOI of < 100). Recombination of the 'floxed' fibronectin gene was verified by allele specific PCR.

Inhibition Experiments. The OvCa cells (SKOV3ip1, HeyA8) were added to a confluent culture of primary human mesothelial cells and treated with the following inhibitors: Rac inhibitor (5μm), Ras inhibitor (25μm), Rho inhibitor (10μm), TGF-βRI inhibitor (10μm) or anti-TGF-βRII (8μg/ml) neutralizing antibody. Fibronectin production and secretion were analyzed, 48h and 72h later, respectively. Fibronectin, Smad3, TGF-βRII and control siRNA constructs were transfected into 2 $x10^6$ primary human mesothelial cells 18h prior to co-culture with SKOV3ip1 cells. SKOV3ip.1 cells were transfected with TGF-β1 or control siRNA constructs using Lipofectamine™ Transfection Reagent (Invitrogen), the cells recovered in full growth media (10% fetal bovine serum) for 18h and serum-free media was added. The OvCa cell (SKOV3ip1, Kuramochi, Tyk-nu, Tyk-nu CP-r, HeyA8) conditioned-media was collected after 48h and concentrated (10x) using a spin column with 3mm filter (Millipore). Eighteen hours after transfection, SKOV3ip1 cells ($1.5x10^6$/well) were trypsinized and added on the transfected mesothelial cells. After 24 hours cells were FACs sorted, RNA isolated and qRT-PCR performed.

TGF-β1 ELISA. A human TGF-β1 immunoassay, Quantikine ELISA (R&D Systems, Inc.), was performed according to manufacturer specifications. Briefly, SKOV3ip1 cells (1x 10^5) and primary human mesothelial cells (2 x 10^5) were cultured alone or co-cultured for 24h in 0.33cm^2 wells.

Rac Activity ELISA. A G-LISA Cdc-42 Activation Assay Biochem Kit (Colorimetric Based) was performed as described by manufacturer specifications (Cytoskeleton, Inc.). Briefly, SKOV3ip1 or HeyA8 cells (1x 10^5) and primary human mesothelial cells (2 x 10^5) were cultured alone or co-cultured for 1, 4, 8, 12 and 24h in 0.33cm^2 wells. Primary human mesothelial cells were treated with epidermal growth factor (10ng/ml) as a positive control.

Australian Ovarian Cancer Study and The Cancer Genome Atlas Data Analysis. The expression of fibronectin mRNA levels was analyzed using a data set composed of the Australian Ovarian Cancer Study (AOCS) cohort (17) or The Cancer Genome Atlas cohort (18). The subtype specific expression level of fibronectin (*Fn1* gene) was analyzed. The expression level of the *Fn1* gene was correlated with the expression level of all the genes in each cohort. When multiple probes map to a gene, the probe with the maximum mean expression level is taken as the representative probe. Genes with a correlation coefficient greater than 0.6 or less than -0.6 and a false discovery rate less than 5% were selected from the cohort. The criteria identified 754 genes in the AOCS cohort (Supplemental Table 1). The list of *Fn1* correlated genes in AOCS cohort were analyzed using GeneGO and 21 molecular pathways were identified at a false discovery rate of less than 5% (Supplemental Table 2).

Treatment Studies. The effect of ATN161 (35, 36) on OvCa cell in vitro invasion and proliferation was investigated . ATN161 (1μg/ml) was added to fluorescently-labeled OvCa cells (SKOV3ip1 and HeyA8) at time of the assay and invasion (24h) and proliferation (96h) assays performed on the pre-plated 3D omental culture (24).

For the *in vivo* intervention study, SKOV3ip1 cells ($1x10^6$) were injected into the peritoneal cavity of athymic nude mice. 7 days after injection the control PBS or ATN161 (1mg/kg/day) were injected three times/week for 3 weeks (10 mice/group). For the prevention study, mice were treated once prior (-4h) to SKOV3ip1 cells ($1x10^6$) injection and twice after inoculation (24h and 72h) with ATN161 (1mg/kg/day). Twenty-

eight days after injection the mice were sacrificed (10 mice/group). The number of tumor colonies was counted and the tumor weighed (50). Procedures involving animal care were approved by the Committee on Animal Care at the University of Chicago.

Statistical Analysis. Proliferation (n=5) assays were performed and at least three independent experiments conducted. The mean and standard error mean (SEM) are reported. Significant changes were determined by two-sided unpaired 2-tailed t-tests, and a P-value <0.05 was considered significant.

Study Approval. Specimens of human omentum were obtained from patients undergoing surgery for benign conditions and tumor samples were collected from ovarian cancer patients undergoing surgery at the University of Chicago. All human specimens were obtained in accordance with a protocol approved by the University of Chicago Institutional Review Board (IRB). All animal procedures were approved by the University of Chicago IACUC and were in accordance with the University of Chicago's policies on the care, welfare and treatment of laboratory animals.

References

1. Brattain M, Brattain D, Fine W, Khaled F, Marks M, Kimball P, Arcolano I, and Danbury B. Initiation and characterization of cultures of human colonic carcinoma with different characteristics utilizing feeder layers of confluent fibroblasts. *OncodevelBiol Med.* 1981;2(355-66.
2. Sawyer JS, Anderson BD, Beight DW, Campbell RM, Jones ML, Herron DK, Lampe JW, McCowan JR, McMillen WT, Mort N, et al. Synthesis and activity of new aryl- and heteroaryl-substituted pyrazole inhibitors of the transforming growth factor-beta type I receptor kinase domain. *J Med Chem.* 2003;46(19):3953-6.
3. Gellibert F, Woolven J, Fouchet MH, Mathews N, Goodland H, Lovegrove V, Laroze A, Nguyen VL, Sautet S, Wang R, et al. Identification of 1,5-naphthyridine derivatives as a novel series of potent and selective TGF-beta type I receptor inhibitors. *J Med Chem.* 2004;47(18):4494-506.
4. Ye X, Wang Y, Rattner A, and Nathans J. Genetic mosaic analysis reveals a major role for frizzled 4 and frizzled 8 in controlling ureteric growth in the developing kidney. *Development.* 2011;138(6):1161-72.
5. George J, Afek A, Keren P, Herz I, Goldberg I, Haklai R, Kloog Y, and Keren G. Functional inhibition of Ras by S-trans,trans-farnesyl thiosalicylic acid attenuates atherosclerosis in apolipoprotein E knockout mice. *Circulation.* 2002;105(20):2416-22.
6. Gao Y, Dickerson JB, Guo F, Zheng J, and Zheng Y. Rational design and characterization of a Rac GTPase-specific small molecule inhibitor. *Proc Natl Acad Sci U S A.* 2004;101(20):7618-23.
7. Sawada K, Radjabi AR, Shinomiya N, Kistner E, Kenny HA, Salgia R, Yamada SD, Vande Woude GF, Tretiakova MS, and Lengyel E. C-Met overexpression is a prognostic factor in ovarian cancer and an effective target for inhibition of peritoneal dissemination and invasion. *Cancer Res.* 2007;67(4):1670-80.
8. Kenny HA, Kaur S, Coussens LM, and Lengyel E. The initial steps of ovarian cancer cell metastasis are mediated by MMP-2 cleavage of vitronectin and fibronectin. *J Clin Invest.* 2008;118(4):1367-79.
9. Kenny HA, Krausz T, Yamada SD, and Lengyel E. Use of a novel 3D culture model to elucidate the role of mesothelial cells, fibroblasts and extra-cellular matrices on adhesion and invasion of ovarian cancer cells. *Int J Cancer.* 2007;121(7):1463-72.
10. Kenny HA, Leonhardt P, Ladanyi A, Yamada SD, Montag AG, Im HK, Jagadeeswaran S, Shaw DE, Mazar AP, and Lengyel E. Targeting the urokinase plasminogen activator receptor inhibits ovarian cancer metastasis. *Clin Cancer Res.* 2011;17(3):459-71.
11. Abberton KM, Bortolotto SK, Woods AA, Findlay M, Morrison WA, Thompson EW, and Messina A. Myogel, a novel, basement membrane-rich, extracellular matrix derived from skeletal muscle, is highly adipogenic in vivo and in vitro. *Cells Tissue Organs.* 2008;188(347-58.
12. Gospodarowicz D, Cheng J, Lui GM, Baird A, and Böhlent P. Isolatin of brain fibroblast growth factor by heparin-sepharose affinity chromatography: I dentitiy with pituitary fibroblast growth factor. *Proceedings of the National Academy of Sciences USA.* 1984;81(6963-7.
13. Pfaffl M. A new mathematical model for relative quantification in real-time RT-PCR. *Nucleic Acids Res.* 2001;29(9):2002-7.
14. Kaur S, Kenny HA, Jagadeeswaran S, Zillhardt M, Montag AG, Kistner E, Yamada SD, Mitra AK, and Lengyel E. ß3-integrin expression on tumor cells inhibits tumor progression, reduces metastasis, and is associated with a favorable prognosis in patients with ovarian cancer. *Am J Pathol.* 2009;175(5):2184-96.
15. Sakai T, Johnson KJ, Muronzono M, Sakai K, Magnuson MA, Wieloch T, Cronberg T, Isshiki A, Erickson HP, and Fässler R. Plasma fibronectin supports neuronal survival and reduces brain injury following transient focal cerebral ischemia but is not essential for skin-wound healing and hemostasis. *Nat Med.* 2001;7(3):324-30.
16. Brunner M, Millon-Frémillon A, Chevalier G, Nakchbandi IA, Mosher D, Block MR, Albigés-Rizo C, and Bouvard D. Osteoblast mineralization requires ß1 integrin/ ICAP-1-dependent fibronectin deposition. *The Journal of Cell Biology.* 2011;194(2):307-22.

17. Tothill RW, Tinker AV, George J, Brown R, Fox SB, Lade S, Johnson DS, Trivett MK, Etemadmoghadam D, Locandro B, et al. Novel molecular subtypes of serous and endometrioid ovarian cancer linked to clinical outcome. *Clin Cancer Res.* 2008;14(16):198-208.
18. The Cancer Genome Atlas N. Integrated genomic analyses of ovarian carcinoma. *Nature.* 2011;474(609-15.

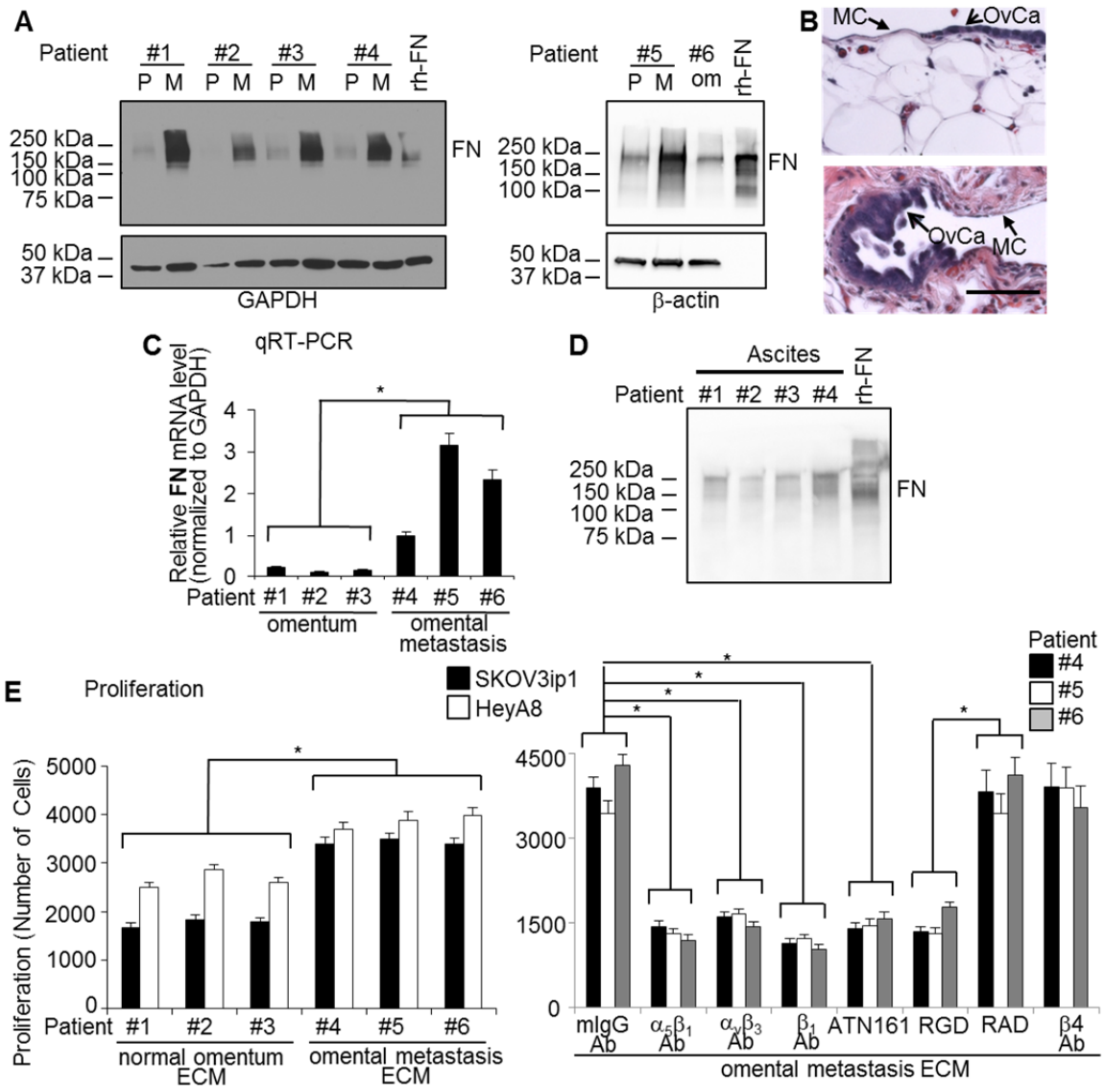

Supplemental Figure 1. High fibronectin expression in ovarian cancer metastasis. (**A**) Immunoblots for fibronectin (FN) in representative tumor samples from five patients (#1-5) with serous papillary ovarian cancer (OvCa, FIGO IIIC) and an omentum sample from one patient without cancer (#6). Fibronectin protein expression was detected in primary tumors (P) and corresponding omental metastases (M) (om, human omental sample from benign patient; rh-FN, recombinant human FN, 80μg). (**B**) Representative images of tissue from a patient incidentally detected with early, microscopic OvCa metastasis to the omentum (FIGO IIIA, representative sections of affected areas; bar, 100μm). Hematoxylin and eosin staining were performed. MC, Mesothelial cells. (**C**) Fibronectin mRNA expression in human omentum and omental metastases samples was examined by qRT-PCR using fibronectin specific probes. (**D**) Immunoblot for FN in ascites samples from four separate patients (#1-4, 10μg of protein, 0.1-0.2μl). Fibronectin protein expression was detected in all ascites samples of serous papillary OvCa patients. 80μg of rh-FN. (**E**) *Left*, proliferation assay (4 days) performed with two ovarian cancer cell lines (SKOV3ip1, HeyA8) on isolated ECM from omental tissue or omental metastasis samples. *Right*, SKOV3ip1 cells were pre-treated for 30 minutes with functional blocking antibodies, a fibronectin fragment (ATN-161), a RGD-peptide or a RAD-peptide. A proliferation assay (72h) was performed on ECM isolated from the omental metastases samples. Each bar is the mean+/- SEM of n=3 (qRT-PCR) or n=5 (proliferation), and is representative of three independent experiments. Two-tailed unpaired student's t test compares the treatments (*, P<0.05).

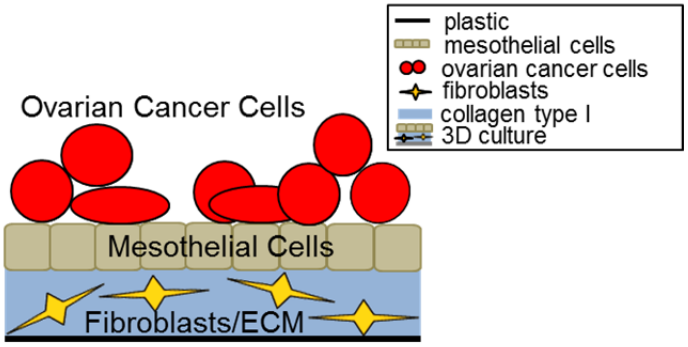

Supplemental Figure 2. **Diagram of mesothelium in a 3D culture.** Primary human omental fibroblasts are plated with human omental ECM and cultured for 4h. The fibroblasts are overlaid with primary human omental mesothelial cells and cultured for an additional 24h before ovarian cancer (OvCa) cells are added to the culture. The 3D culture is utilized to investigate OvCa cell adhesion (30 min), invasion (24h) and proliferation (72 h).

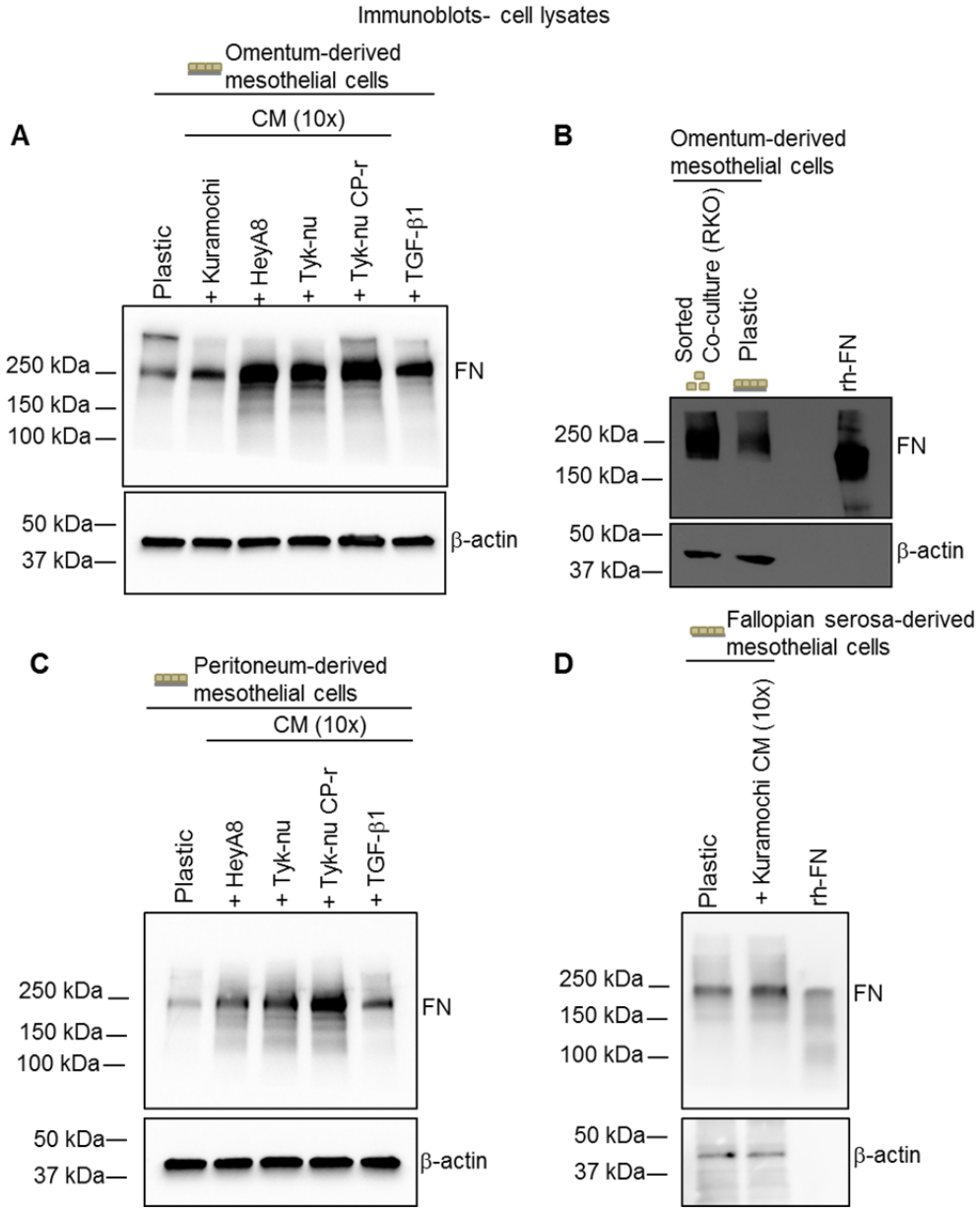

Supplemental Figure 3. **Numerous tumor cells induce fibronectin expression in mesothelial cells collected from various anatomic sites in the peritoneal cavity.** Immunoblots for fibronectin. Detection of fibronectin (FN) produced in primary human (**A-B**) omentum-derived, (**C**) peritoneum-derived, or (**D**) fallopian serosa-derived mesothelial cells. (**B**) Mesothelial cells were cultured on plastic or co-cultured (48h) with colon cancer cells (RKO) and separated by fluorescently-activated cell sorting. (**A, C, D**) Mesothelial cells were treated with ovarian cancer cell conditioned media (CM) or TGF-β for 72h and cell lysates extracted (rh-FN, recombinant human FN).

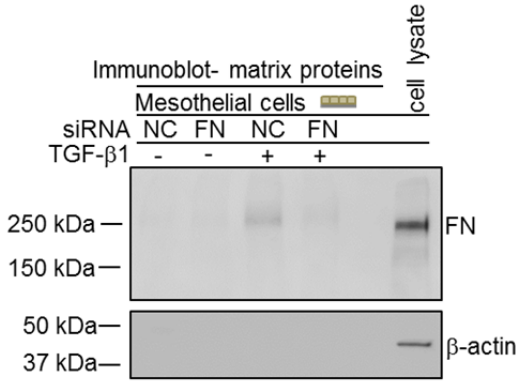

Supplemental Figure 4. **Inhibiting fibronectin in primary human mesothelial cells by siRNA decreases fibronectin (FN) secretion.** Immunoblot analysis of fibronectin secreted by primary human mesothelial cells. Primary human mesothelial cells were transfected with fibronectin (FN) specific or negative control (NC) siRNA 24h prior to treatment with TGF-β1 for 48h.

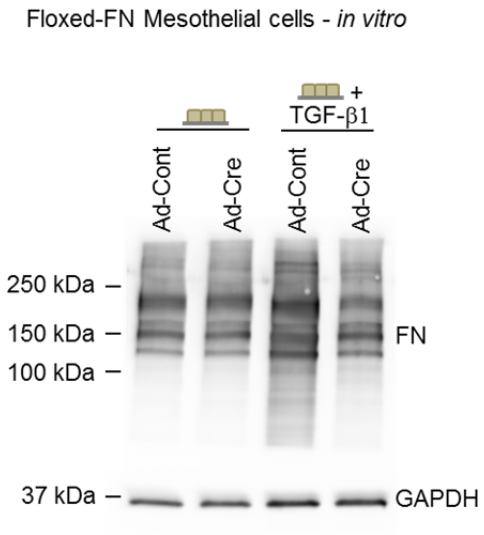

Supplemental Figure 5. Genetic knock-down of fibronectin. Knock-down of fibronectin (FN) in primary mouse mesothelial cells from *Fibronectin1* floxed mice (*FN*$^{fl/fl}$). Immunoblot analysis of FN in mesothelial cells isolated from *FN*$^{fl/fl}$ mice. The mesothelial cells were treated for 72h with either empty adenovirus (Ad-Cont) or Cre recombinase containing adenovirus (Ad-Cre) to delete the fibronectin gene, followed by treatment with or without TGF-β1 for 48h (rh-FN, recombinant human FN).

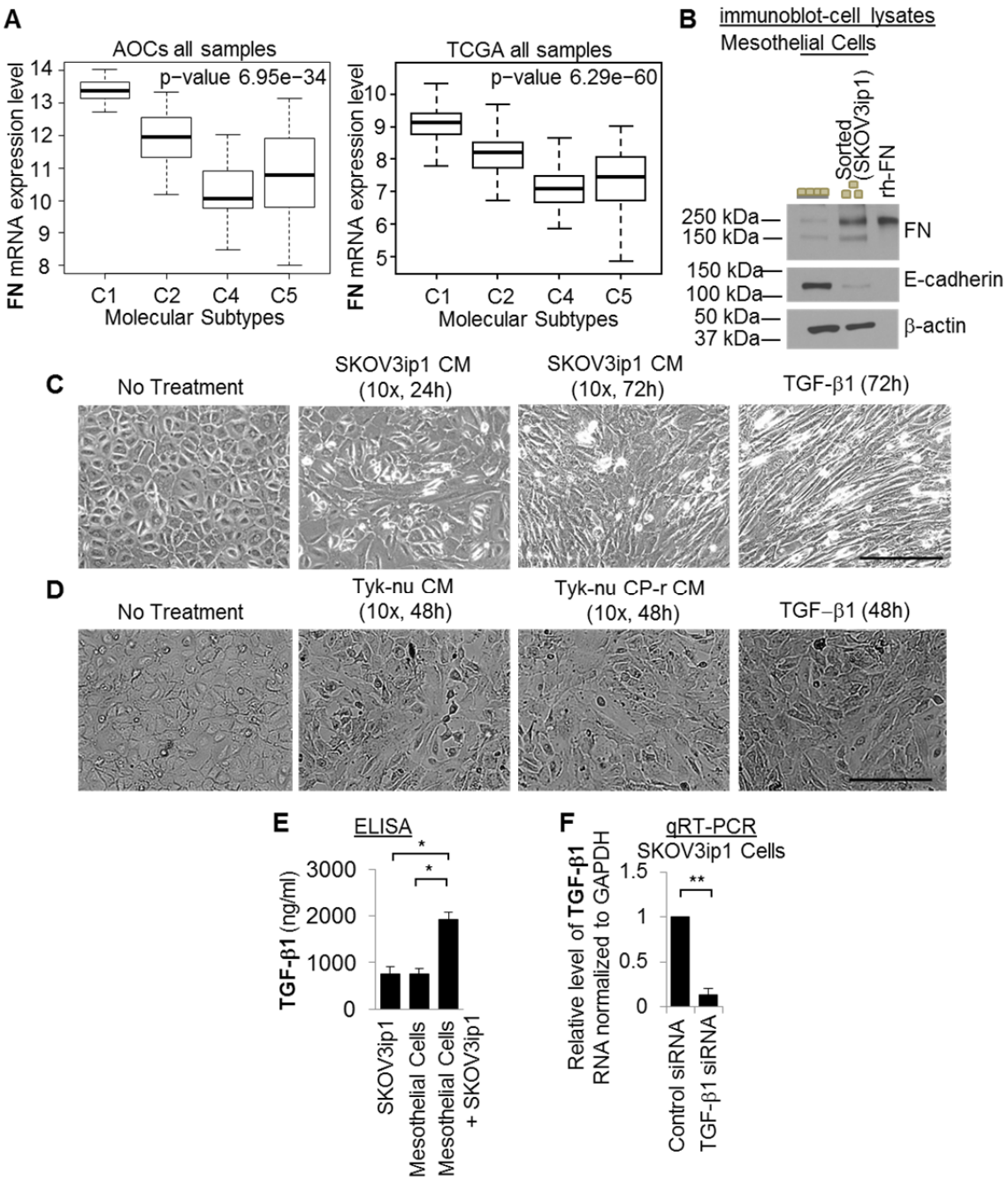

Supplemental Figure 6. **Tumor cells induce a mesenchymal phenotype in primary human mesothelial cells.** (**A**) mRNA levels of fibronectin expression in high-grade serous ovarian cancer (OvCa) from the (*left*) Australian OvCa Study (AOCS) and the (*right*) the Cancer Genome Atlas (TCGA). Box-plot depicting the relationship between fibronectin (FN) expression and molecular subtype. Minimum and maximum fibronectin expression are depicted by black dots, the box signifies the upper and lower quartiles, and the median is represented by a short black line within the box. A Wilcoxon rank test compares the treatments (median+/-1.5 interquartile range; ***P<0.001; bar, 100μm. Four molecular subtypes of ovarian cancer expressed high levels of fibronectin, including the C1 (high stromal response), C2 (high immune signature), C4 (low stromal response), and C5 (mesenchymal, low immune signature) subtypes; all of which are associated with high grade serous cancer. The molecular subtype with the highest level of fibronectin expression, C1, was the subtype

associated with the significantly poorest survival. (**B**) Immunoblot analysis of fibronectin and E-cadherin protein expression in cell lysates of primary human mesothelial cells grown on plastic and in co-culture with SKOV3ip1 cells for 48h after separation by fluorescently-activated cell sorting (rh-FN, recombinant human FN). (**C**) Concentrated (10x) SKOV3ip1 OvCa cell conditioned media (CM) stimulates a mesenchymal-like morphology change in primary human mesothelial cells within 72h. Phase-contrast pictures of primary human mesothelial cells treated with or without concentrated (10x) SKOV3ip1 CM (24h or 72h). Bar = 100μm. (**D**) Concentrated (10x) Tyk-nu and Tyk-nu CP-r OvCa cell CM stimulates a mesenchymal-like morphology change in primary human mesothelial cells within 48h. Phase-contrast pictures of primary human mesothelial cells treated with or without concentrated (10x) OvCa CM (48h). Bar = 100μm. (**E**) Increased levels of TGF-β1 are secreted when ovarian cancer cells are co-cultured with primary human mesothelial cells. SKOV3ip1 cells and primary human mesothelial cells were grown on plastic or in co-culture and TGF-β1 levels measured using a TGF-β1 ELISA. (**F**) Knock-down of TGF-β1 in SKOV3ip1 cells. SKOV3ip1 cells were transfected with control or TGF-β1 specific siRNA . RNA was isolated after 24h, and TGF-β1 mRNA levels were analyzed by qRT-PCR. Each bar is the mean+/- SEM of n=5 (ELISA) or n=3 (qRT-PCR), and is representative of three independent experiments. Two-tailed unpaired Student's t test compares the treatments (*, $P<0.05$, **, $P<0.01$).

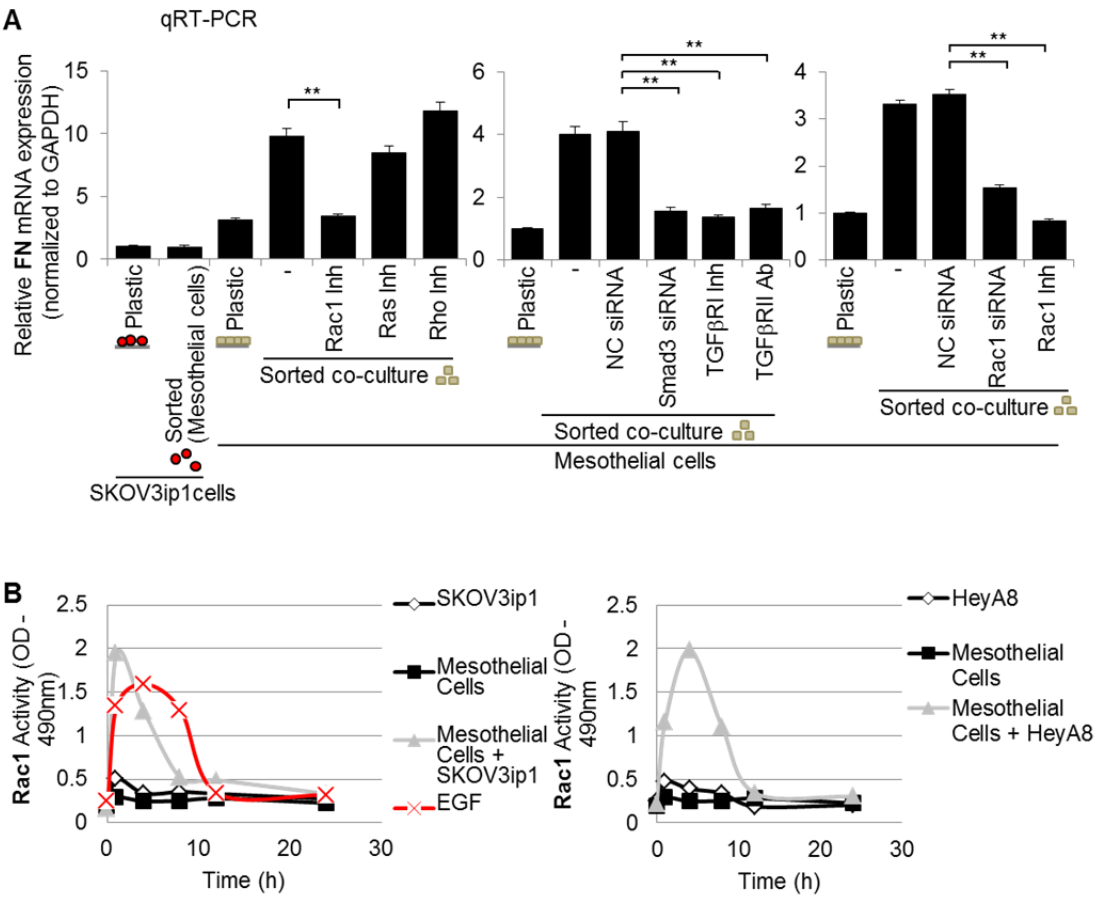

Supplemental Figure 7. **Tumor cells induce fibronectin mRNA expression in mesothelial cells through a TGF-β1/Smad3/Rac1 dependent signaling pathway.** (**A**) Primary human mesothelial cells were transfected with a negative control (NC) or Rac1 specific siRNA (48h) and immunoblot analysis for Rac1 performed. Primary human mesothelial cells were transfected with a negative control (NC), Smad3 or TGF-βRII specific siRNA (24h) and qRT-PCR analysis of Smad3 and TGF-βRII mRNA performed. Fibronectin (FN) mRNA expression in the ovarian cancer cell line SKOV3ip1 and primary human mesothelial cells on plastic or in co-culture in the presence of various inhibitors after separation by fluorescently-activated cell sorting (FACs). qRT-PCR analysis of fibronectin mRNA expression was performed. Primary human mesothelial cells were transfected with a negative control (NC), Smad3 or Rac1 siRNA (18h) and co-cultured with SKOV3ip1 cells or treated with inhibitors (Rac1 inhibitor, Ras inhibitor, Rho inhibitor, TGF-βRI inhibitor or TGF-βRII antibody) when co-cultured with SkVO3ip1 cells (24h) followed by FACs, RNA extraction and qRT-PCR analysis. Each bar is the mean+/- SEM of n=3, and is representative of three independent experiments. Two-tailed unpaired Student's t test compares the treatments (**, P<0.01). (**B**) Increase in Rac1 activity when OvCa cells are co-cultured with primary human mesothelial cells. Rac1 activity (Rac1-GTP levels) was detected over time using a Rac 1 G-LISA in cultures of primary human mesothelial cells, OvCa cells (SKOV3ip1, *left* and HeyA8, *right*) or both co-cultured. Epidermal growth factor (EGF) treatment of mesothelial cells is the positive control.

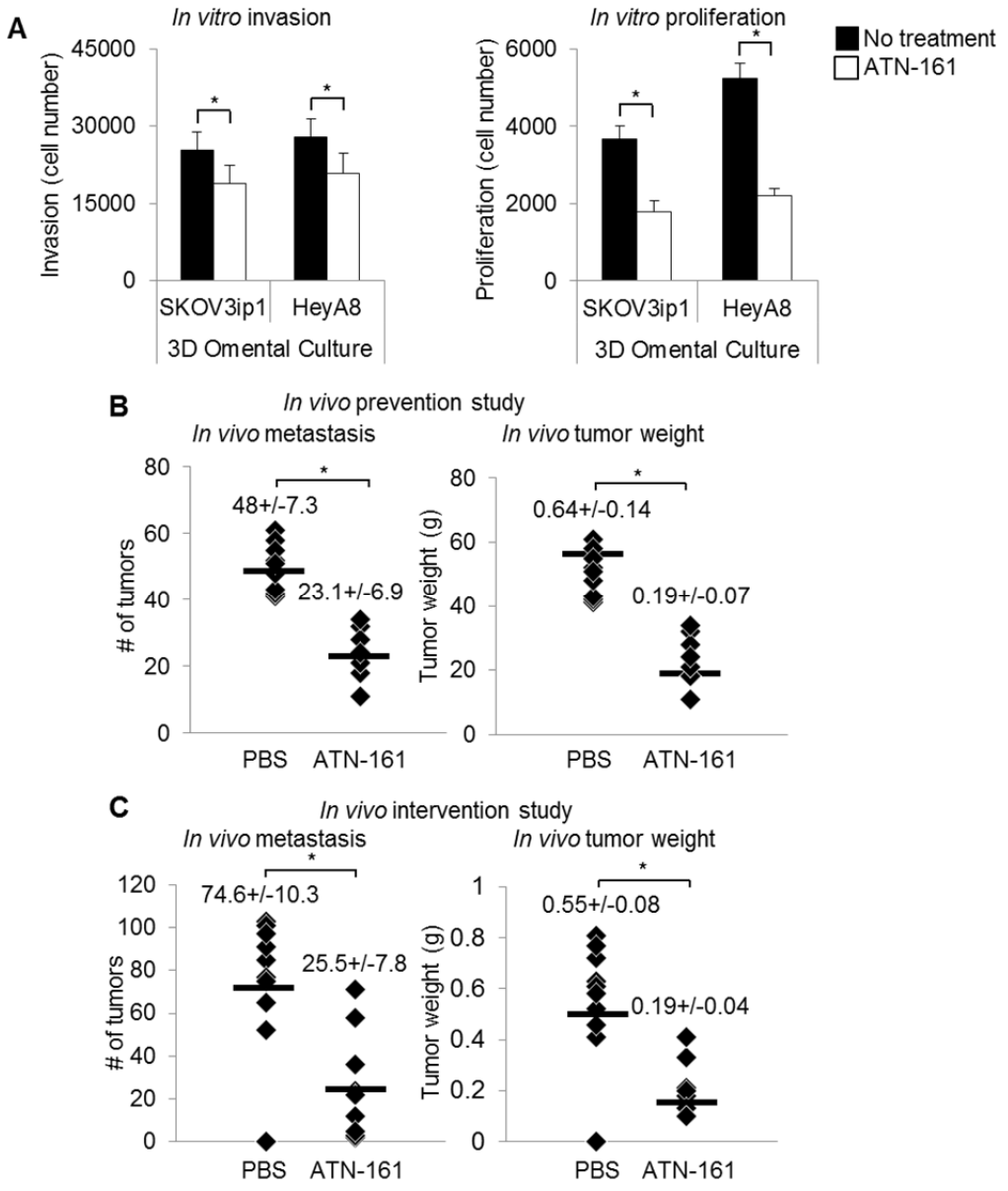

Supplemental Figure 8. A fibronectin peptide blocks ovarian cancer cell metastasis. (**A**) In vitro testing of the fibronectin (FN) inhibitor, ATN-161, a peptide derived from the synergy region of fibronectin. Invasion (24h) and proliferation (96h) of OvCa cells (HeyA8, SKOV3ip1) to the 3D omental culture (mean+/- SD; n=3 (invasion); n=5 (proliferation); three independent experiments *P<0.05). (**B-C**) In vivo testing of ATN-161 using the SKOV3ip1 xenograft model of OvCa metastasis. (**B**) Prevention study. Mice were treated once prior to SKOV3ip1 i.p. injection and two times after inoculation with ATN-161 (1 mg/kg/day on days 3 and 5). (**C**) intervention study. Mice were treated 3 times/week with ATN-161 (1 mg/kg/day) for 3 weeks, starting 7 days post SKOV3ip1 i.p. injection. Each point represents the number of metastatic tumors (*left*) or tumor weight (*right*) 28 days post injection. Lines are the means of treatment groups and values defined, *P<0.05.

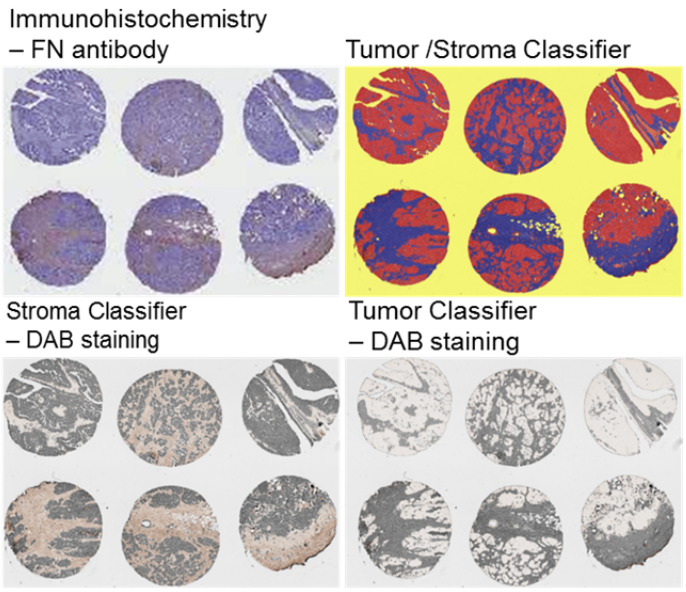

Supplemental Figure 9. **Analysis of fibronectin protein expression and localization in tumor and stromal regions of serous papillary ovarian cancer metastatic tumors.** Immunohistochemical analysis using a fibronectin (FN) specific antibody in tissue microarrays representing the omental metastases of 108 patients. Tumor and stroma specific classifiers were developed using Aperio's Spectrum Analysis Program with Genie capabilities. The intensity of DAB staining was determined in the tumor or stroma specific regions of the tumor cores.

Supplemental Table 1. Genes with expression levels significantly correlated (R>0.60) with that of *f*ibronectin (FN1) in Australian Ovarian Cancer Study and The Cancer Genome Atlas (false discovery rate of <5%).

		Corr. Coeff.	
	Gene Symbol	**AOCS**	**TCGA**
1	FN1	1.00	1
2	THBS2	0.91	0.87
3	VCAN	0.90	0.84
4	INHBA	0.90	0.77
5	FAP	0.90	0.81
6	COL5A2	0.90	0.84
7	PRRX1	0.89	0.81
8	COL5A1	0.88	0.79
9	POSTN	0.87	0.74
10	LOX	0.87	0.8
11	ADAM12	0.87	0.8
12	CTHRC1	0.86	0.77
13	COL11A1	0.86	0.77
14	CTSK	0.86	0.74
15	FBN1	0.86	0.74
16	SPARC	0.85	0.79
17	SERPINF1	0.85	0.8
18	TNFAIP6	0.84	0.73
19	COL8A1	0.84	0.72
20	PLAU	0.84	0.72
21	COL3A1	0.84	0.77
22	RAB31	0.84	0.81
23	ACTA2	0.83	0.76
24	ADAMTS12	0.83	0.77
25	SNAI2	0.83	0.74
26	AEBP1	0.82	0.75
27	MMP2	0.82	0.74
28	PMP22	0.82	0.76
29	LUM	0.82	0.74
30	OLFML2B	0.81	0.72
31	BGN	0.81	0.73
32	TMEM158	0.80	0.7
33	DSE	0.80	0.71
34	ANTXR1	0.80	0.7
35	ISM1	0.79	0.8
36	PDLIM3	0.79	0.71
37	LOXL2	0.78	0.7
38	PMEPA1	0.77	0.7
39	ANGPTL2	0.76	0.7
40	WISP1	0.76	0.7
		Corr. Coeff.	

Supplemental Table 2
Significant biological pathways identified using GeneGO that correlate with fibronectin expression in Australian Ovarian Cancer Study (false discovery rate<5%).

	Maps	p-value
1	Cell adhesion ECM remodeling	3.74E-14
2	Development Regulation of epithelial-to-mesenchymal transition (EMT)	6.40E-10
3	Cell adhesion Chemokines and adhesion	2.30E-08
4	Development TGF-beta-dependent induction of EMT via SMADs	6.70E-07
5	Development TGF-beta-dependent induction of EMT via RhoA, PI3K and ILK	2.70E-06
6	Cytoskeleton remodeling Role of Activin A in cytoskeleton remodeling	1.20E-04
7	Cytoskeleton remodeling Cytoskeleton remodeling	1.40E-04
8	Cytoskeleton remodeling TGF, WNT and cytoskeletal remodeling	2.00E-04
9	Cell adhesion Endothelial cell contacts by non-junctional mechanisms	2.10E-04
10	Cell adhesion Plasmin signaling	6.60E-04
11	Hypoxia-induced EMT in cancer and fibrosis	8.40E-04
12	Development TGF-beta-dependent induction of EMT via MAPK	1.60E-03
13	Cell adhesion Integrin-mediated cell adhesion and migration	1.70E-03
14	Cytoskeleton remodeling Integrin outside-in signaling	1.80E-03
15	Some pathways of EMT in cancer cells	2.00E-03
16	Transport Macropinocytosis regulation by growth factors	3.60E-03
17	Development NOTCH-induced EMT	3.90E-03
18	Chemotaxis Leukocyte chemotaxis	5.90E-03
19	Cytoskeleton remodeling Role of PDGFs in cell migration	6.10E-03
20	Neurophysiological process Dopamine D2 receptor transactivation of PDGFR in CNS	7.20E-03
21	Development S1P2 and S1P3 receptors in cell proliferation and differentiation	7.20E-03

Supplemental Table 3

Fibronectin expression in the tumor and stromal components of human ovarian cancer.

		Total number (%)	Tumor FN ≤ Median	Tumor FN > Median	Tumor FN P-value	Stroma FN ≤ Median	Stroma FN > Median	Stroma FN P-value
Ovarian cancer stage					0.42			0.72
	IIIA	1 (0.9)	1	0		0	1	
	IIIB	6 (5.6)	4	2		4	2	
	IIIC	73 (67.6)	33	40		37	36	
	IV	28 (25.9)	16	12		13	15	
Cytology					0.37			0.18
	Positive/Atypical	77 (71.3)	36	41		42	35	
	Negative	5 (4.6)	4	1		3	2	
	Not Done	26 (24.1)	14	12		9	17	
Ascites volume					1.00			0.42
	No	42 (42)	21	21		23	19	
	Yes	58 (58)	28	30		26	32	
Chemotherapy					0.35			0.82
	Gemcitabine	1 (0.9)	1	0		1	0	
	Other/Platinum	1 (0.9)	1	0		0	1	
	Platinum only	3 (2.9)	3	0		1	2	
	Taxane	1 (0.9)	0	1		1	0	
	Taxane/Platinum	96 (91.4)	47	49		49	47	
	Other	3 (2.9)	2	1		1	2	
Grading					0.20			0.09
	G1	2 (1.9)	0	2		0	2	
	G2	28 (25.9)	17	11		18	10	
	G3	78 (72.2)	37	41		36	42	
Tumor site					0.49			0.40
	1	88 (82.2)	46	42		47	41	
	2	2 (1.9)	1	1		1	1	
	3	17 (15.9)	6	11		6	11	
Platinum					0.11			0.31
	Sensitivity	49 (46.7)	28	21		22	27	
	Resistant	31 (29.5)	11	20		15	16	
	Sensitive	25 (23.8)	15	10		16	9	
	Intermediate							
CA125					0.82			0.82
	≤200	27 (30.7)	14	13		14	13	
	>200	61 (69.3)	29	32		34	27	
Residual tumor					0.56			0.05
	> 1cm	55 (51.4)	26	29		22	33	
	≤ 1cm	52 (48.6)	28	24		31	21	
Chemotherapy type					0.41			0.27
	Adjuvant/1st line	90 (85.7)	48	42		43	47	
	Neoadjuvant	15 (14.3)	6	9		10	5	

NOTE: Clinical data of patients with advanced stage serous papillary ovarian cancer (n=108). Immunohistochemistry was performed using a fibronectin specific antibody, and the protein expression levels and pattern were analyzed in tumor and stromal cells of omental metastases using specific algorithms to identify tumor and surrounding stroma with the Aperio ImageScope and Spectrum software.